Hindawi Publishing Corporation
Journal of Nanomaterials
Volume 2014, Article ID 972475, 8 pages
http://dx.doi.org/10.1155/2014/972475

Research Article

Organic-Inorganic Hybrid Hollow Mesoporous Organosilica Nanoparticles for Efficient Ultrasound-Based Imaging and Controlled Drug Release

Xiaoqin Qian,[1,2] Wenping Wang,[1] Wentao Kong,[1] and Yu Chen[3]

[1] *Department of Ultrasound, Zhongshan Hospital, Fudan University, Shanghai 200050, China*
[2] *The First People's Hospital of Zhenjiang City, Zhenjiang 212002, China*
[3] *State Key Laboratory of High Performance Ceramics and Superfine Microstructure, Shanghai Institute of Ceramics, Chinese Academy of Sciences, Shanghai 200050, China*

Correspondence should be addressed to Wenping Wang; puguang61@126.com and Yu Chen; chenyu@mail.sic.ac.cn

Received 17 January 2014; Accepted 15 May 2014; Published 24 June 2014

Academic Editor: Hongchen Chen Gu

A novel anticancer drug delivery system with contrast-enhanced ultrasound-imaging performance was synthesized by a typical hard-templating method using monodispersed silica nanoparticles as the templates, which was based on unique molecularly organic/inorganic hybrid hollow periodic mesoporous organosilicas (HPMOs). The highly dispersed HPMOs show the uniform spherical morphology, large hollow interior, and well-defined mesoporous structures, which are very beneficial for ultrasound-based theranostics. The obtained HPMOs exhibit excellent performances in contrast-enhanced ultrasonography both *in vitro* and *in vivo* and can be used for the real-time determination of the progress of lesion tissues during the chemotherapeutic process. Importantly, hydrophobic paclitaxel- (PTX-) loaded HPMOs combined with ultrasound irradiation show fast ultrasound responsiveness for controlled drug release and higher *in vitro* and *in vivo* tumor inhibition rates compared with free PTX and PTX-loaded HPMOs, which is due to the enhanced ultrasound-triggered drug release and ultrasound-induced cavitation effect. Therefore, the achieved novel HPMOs-based nanoparticle systems will find broad application potentials in clinically ultrasound-based imaging and auxiliary tumor chemotherapy.

1. Introduction

Ultrasound (US) imaging is one of the most used diagnostic modalities clinically with the unique noninvasive, nonionizing, real-time, and economic features [1]. However, its imaging resolution and diagnostic precision are still much lower than clinical magnetic resonance, computed tomography, and positron emission tomography imaging [2]. The employment of ultrasound contrast agents (CAs) has been demonstrated as an alternative approach to improve the diagnostic precision of ultrasonography because the elaborately designed CAs can act as the efficient reflectors for ultrasound [3–6]. However, the traditional organic microbubbles-based CAs exhibit the extremely large particle sizes (typically in micrometers) and show low stability under ultrasound irradiation, which severely restricts their further clinical applications [1, 7].

Recent preliminary results have demonstrated that hollow silica nanoparticles (NPs) with large hollow interiors and thin shells exhibited satisfactory echogenic properties and excellent ultrasound imaging performances due to their hollow nanostructures, tunable particulate sizes, high stability, and easy surface functionalization [7–10]. To further explore the ultrasound-based diagnostic and therapeutic applications of silica-based NPs, we herein for the first time elaborately designed and fabricated special hollow periodic mesoporous organosilica nanoparticles (HPMOs) with organic/inorganic hybrid features, which function as the CAs for ultrasound imaging and carriers for *in vitro* and *in vivo* ultrasound-based drug release/delivery simultaneously. The fabricated HPMOs possess the unique structural and compositional characteristics for ultrasound-based theranostics. Firstly, the hollow nanostructures and nanoparticulate sizes endow HPMOs

with the excellent echogenic properties and enhanced drug-loading capacity [11–21]. Secondly, the porous HPMOs' shell provides the channels for the free diffusion and encapsulation of drug molecules [22, 23], and hydrophobic antitumor drug paclitaxel- (PTX-) loaded HPMOs combined with ultrasound irradiation show fast ultrasound responsiveness for controlled drug release. Thirdly, their small particle size can enter the tumor tissue through the gap of the tumor capillary, which is difficult to be realized based on traditional organic microbubbles. Importantly, the organic/inorganic hybrid compositions further guarantee the higher biosafety of HPMOs than that of traditional silica NPs with pure Si–O–Si bonds [24]. Based on the well-defined and highly dispersed HPMOs, their theranostic functions for ultrasound-based imaging and therapy have been systematically investigated both *in vitro* and *in vivo*.

2. Experimental Section

2.1. Synthesis of HPMOs. HPMOs were prepared by a special templating method based on a chemical etching process in alkaline solution. Typically, 74 mL of ethanol, 10 mL of H_2O, and 3.14 mL of ammonia (36%–38%) solution were mixed followed by addition of 6 mL of tetraethyl orthosilicate (TEOS) at 30°C. After further 1-hour reaction, the preformed silica NPs were dropped into a mixture containing 100 mL of H_2O, 30 mL of cetyltrimethylammonium bromide (C_{16}TAB) solution, and 3 mL of ammonia solution. 3 mL of 1,4-bis(triethoxysilyl)benzene (BTEB) was then injected into the above solution dropwise followed by 6-hour reaction at 30°C under magnetic stirring. The core/shell structured SiO_2@PMOs were collected by centrifugation, which were further etched in 0.6 M Na_2CO_3 solution at 80°C for 1 h. Finally, the surfactant C_{16}TAB was removed by extraction in HCl solution for three times at 80°C. The products were washed three times by water and ethanol and were finally freeze-dried.

2.2. Contrast-Enhanced Ultrasonography of HPMOs In Vitro. The *in vitro* contrast-enhanced ultrasound imaging was conducted using PTX-HPMOs PBS solutions with different concentrations (2 mL : 5 mg/mL, 10 mg/mL, and 20 mg/mL) by wrapping them into a small sac, which was further infused into a big sac prefilled with PBS solution. The performance of HPMOs as contrast agents for ultrasonography was compared with commercial SonoVue (2 mL). The *in vitro* ultrasonography experiment was carried out on IU-22. In addition, different ultrasound imaging modalities (contrast and harmonic modes) and different mechanical indexes (MI, 0.05–1.2) were employed to systematically investigate the influence of parameters for ultrasound imaging. The corresponding average gray values were determined by the analysis with SONOMATH-DICOM software.

2.3. PTX Loading into HPMOs (PTX-HPMOs) and the Releasing Performance. The PTX-HPMOs were obtained by mixing 5.0 mg of HPMOs with 3 mg of PTX (in 6 mL DMSO solution) at room temperature in the dark, and the mixture was then stirred for 24 h. The supernatant PTX solutions were collected by centrifugation, and the concentration of unloaded PTX was measured. The PTX solutions before and after the coincubation with HPMOs were analyzed by UV-Vis analysis.

PTX-loaded HPMOs (5 mg) were added into the dialysis bag and then introduced into a vial with PBS (50 mL) with or without ultrasound irradiation. Firstly, the medium was stirred at 110 ± 4 revolutions/min at 37 ± 0.5°C without ultrasound irradiation. At the indicated time intervals (observed until 72 h), the medium was removed (5 mL) and replaced with fresh PBS (5 mL). The absorbance intensity of samples of the replaced media was detected by a UV spectrophotometer at wavelength of 233 nm. The released PTX in these replaced media at different time intervals was calculated from the standard curve. Then, ultrasound irritation was applied at 1 h, 3.5 h, and 5.5 h to the PTX-loaded HPMOs, respectively. The parameters of ultrasound irradiation are listed as follows: frequency of 1 MHz, 50% duty cycle, ultrasound power of 1.5 W/cm^2, irradiation duration of 15 s with 5 s pause. The whole irradiation time lasted for 2 min each time.

2.4. Evaluation of the Antitumor Activity of Ultrasound-Mediated PTX-HPMOs In Vitro. The evaluation is based on the typical CCK8 assay. Typically, HeLa cancer cells were seeded in 96-well plate at a density of 3×10^3 cells in 200 μL Dulbecco's modified Eagle's medium (DMEM) containing 10% (v/v) FBS (fetal bovine serum), penicillin (100 IU/mL), and streptomycin (100 μg/mL) in a humidified incubator at 37°C, 5% CO_2 for 12 h. Then, each treatment was carried out as follows: free PTX group was adding the medium with different concentrations (0, 2.5, 5, and 10 μg/mL) of free PTX into the 96-well plate; PTX-HPMOs group was adding the PTX-HPMOs of the same PTX-equivalent doses, without ultrasound irradiation; PTX-HPMOs + US group was adding the PTX-HPMOs of the same PTX-equivalent doses combined with ultrasound irradiation; and, in control group, new DMEM was added. Optical microscope was used to observe the cell growth and morphology in the culture plate after the cells were cultured for 24 h. After extraction of medium in wells, CCK-8 was used to determine the cell survival. The absorbance was measured at 450 nm using a microtiter plate reader (Thermomax microplate reader, Molecular Devices). Consider the following: cell viability (%) = mean OD value of experimental group/mean OD value of control group × 100%. The ultrasound parameters are power: 1.5 W/cm^2, frequency: 1 MHz, duty cycle: 20%, and irradiation time: 2 min with 15 s interval/5 s pause.

2.5. Evaluation of the Antitumor Activity of Ultrasound-Mediated PTX-HPMOs In Vivo. The antitumor activity of ultrasound-mediated PTX-HPMOs-treated tumor was evaluated using nude mice implanted with a human cervical cancer HeLa cell line. Animal procedures were in agreement with the guidelines of the Institutional Animal Care and Use Committee. 200 μL of 2×10^6 tumor cells was inoculated at a subcutaneous (s.c.) site in the armpit of right anterior limb of BALB/c female nude mice aged 5 weeks and fed under

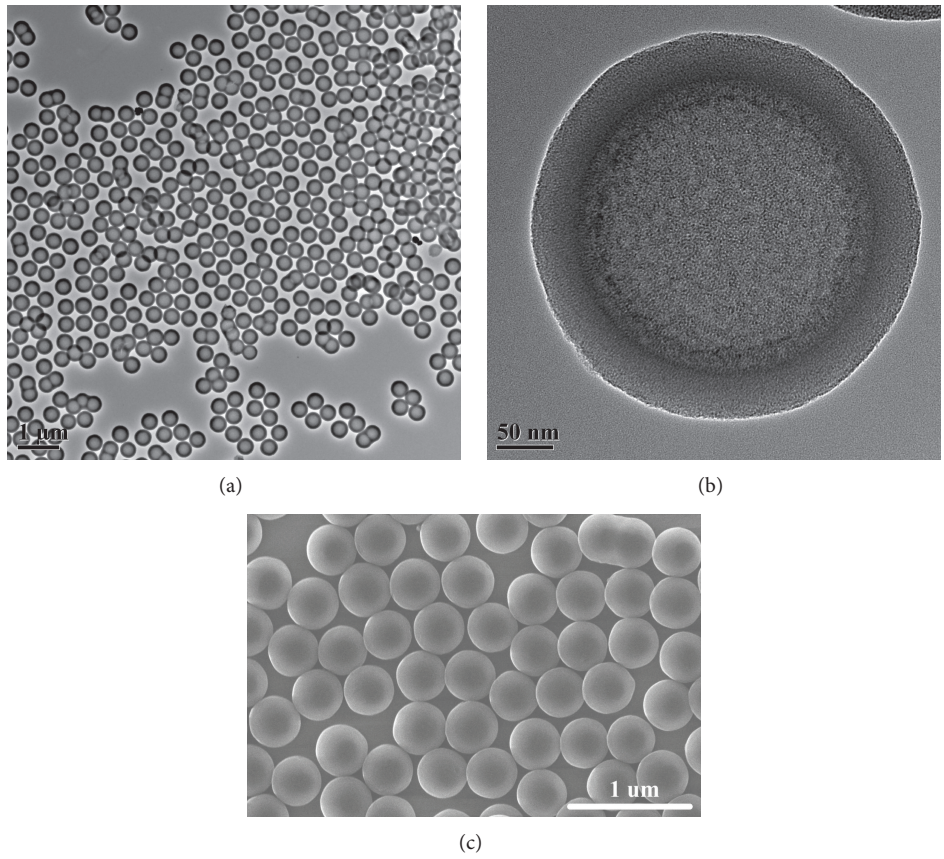

(a) (b)

(c)

Figure 1: TEM (a and b) and SEM (c) images of HPMOs obtained by alkaline etching in 0.6 M Na_2CO_3 solution at 80°C for 1 h.

the condition of SPF. Treatments were started after 2 weeks when tumor in the nude mice reached a tumor volume of 10–15 mm^3. Mice were randomly divided into four groups: (i) PTX administration group, (ii) PTX-HPMOs administration group, (iii) PTX-HPMOs + US administration group, and (iv) control administration group. Each treatment was carried out as follows: PTX group was injected intratumorally at a dose of 200 μL (the actual dose was 300 μg and drug concentration was 1.5 mg/mL). The administration dose is calculated to be 10 mg/kg. PTX-HPMOs administration group was injected intratumorally with the same PTX-equivalent doses without ultrasound irradiation; PTX-HPMOs + US administration group was injected intratumorally with the same PTX-equivalent doses with ultrasound irradiation; and, in control group, animals were given saline. Mice were treated weekly for 3 weeks. The PTX-HPMOs-treated tumor was exposed to US at a power intensity of 1 MHz, 50% duty cycle, sound intensity of 1.5 W/cm^2, and continued irradiation of 2 minutes.

The antitumor effect was assessed by measuring the tumor size at two-day intervals. Tumor volume was calculated by the formula $V = 1/2 \times a \times b \times c$ (where a is the longest diameter of tumor, b is the minor diameter of tumor, and c is the tumor thickness measurement with ultrasound). The inhibition rate of tumor weight is the following: % = [1 − average tumor weight of experimental group/average tumor weight of control group] × 100%.

2.6. Contrast-Enhanced Ultrasonography of PTX-HPMOs In Vivo. SonoVue freeze-dried powder containing 59 mg SF_6 was diluted to 12 mg/mL with 0.9% saline solution before using Mindray M7 series 10 MHz. Animal procedures were in agreement with the guidelines of the Institutional Animal Care and Use Committee. 200 μL of 2×10^6 tumor cells was inoculated at a subcutaneous (s.c.) site in the armpit of right anterior limb of BALB/c female nude mice aged 5 weeks and raised under the condition of SPF. Treatments were started after 2 weeks when tumor in the nude mice reached a tumor volume of 10–15 mm^3. The first group of mice as a control was injected intratumorally at a dose of 200 μL saline. The second group of mice was given 200 μL of commercial SonoVue, and the third group of mice was injected intratumorally at a dose of 200 μL of PTX-HPMOs (the drug diluted with saline to the concentration was 1.5 mg/mL). The ultrasound imaging of tumor tissues was obtained immediately, after 30 s, and after 7 days, respectively.

3. Results and Discussion

HPMOs were synthesized by a typical hard-templating method based on the stability variations of silica core (template) and PMOs shell [25]. The core/shell structured SiO_2@PMOs were firstly prepared by coating a PMOs shell onto the surface of as-prepared silica NPs using BTEB as

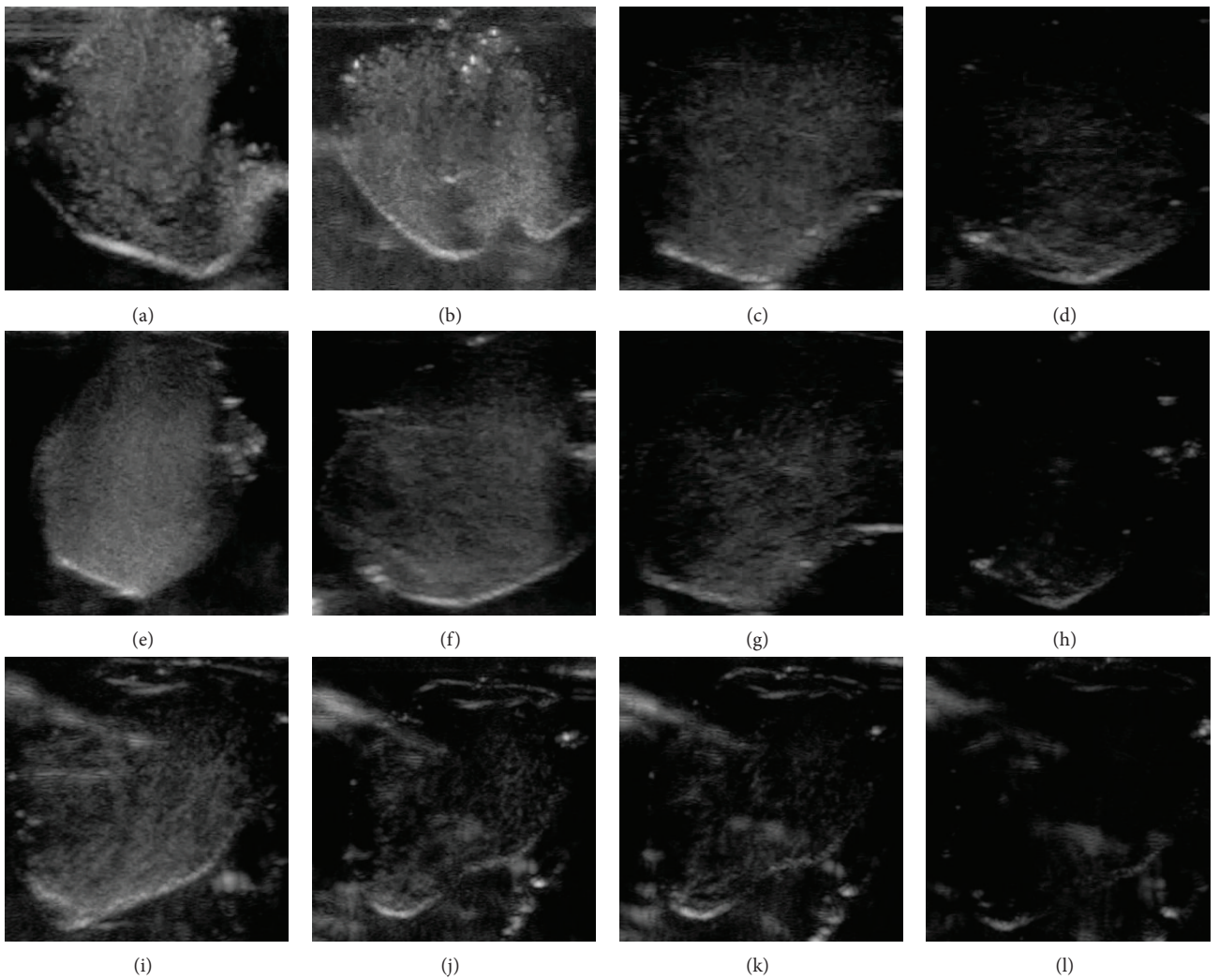

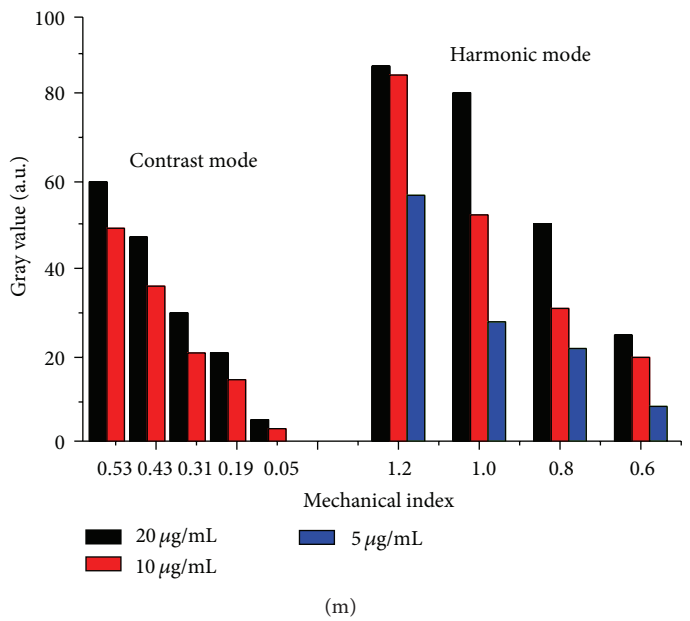

(m)

Figure 2: *In vitro* ultrasonographic images of HPMO NPs of harmonic mode at different concentrations ((a)–(d): 20 mg/mL; (e)–(h): 10 mg/mL; (i)–(l): 5 mg/mL) and different mechanical indexes ((a), (e), and (i): 1.2; (b), (f), and (j): 1.0; (c), (g), and (k): 0.8; (d), (h), and (l): 0.6). (m) The *in vitro* acoustic signal intensities (gray value) of HPMOs solutions under different imaging modes, concentrations, and mechanical indexes.

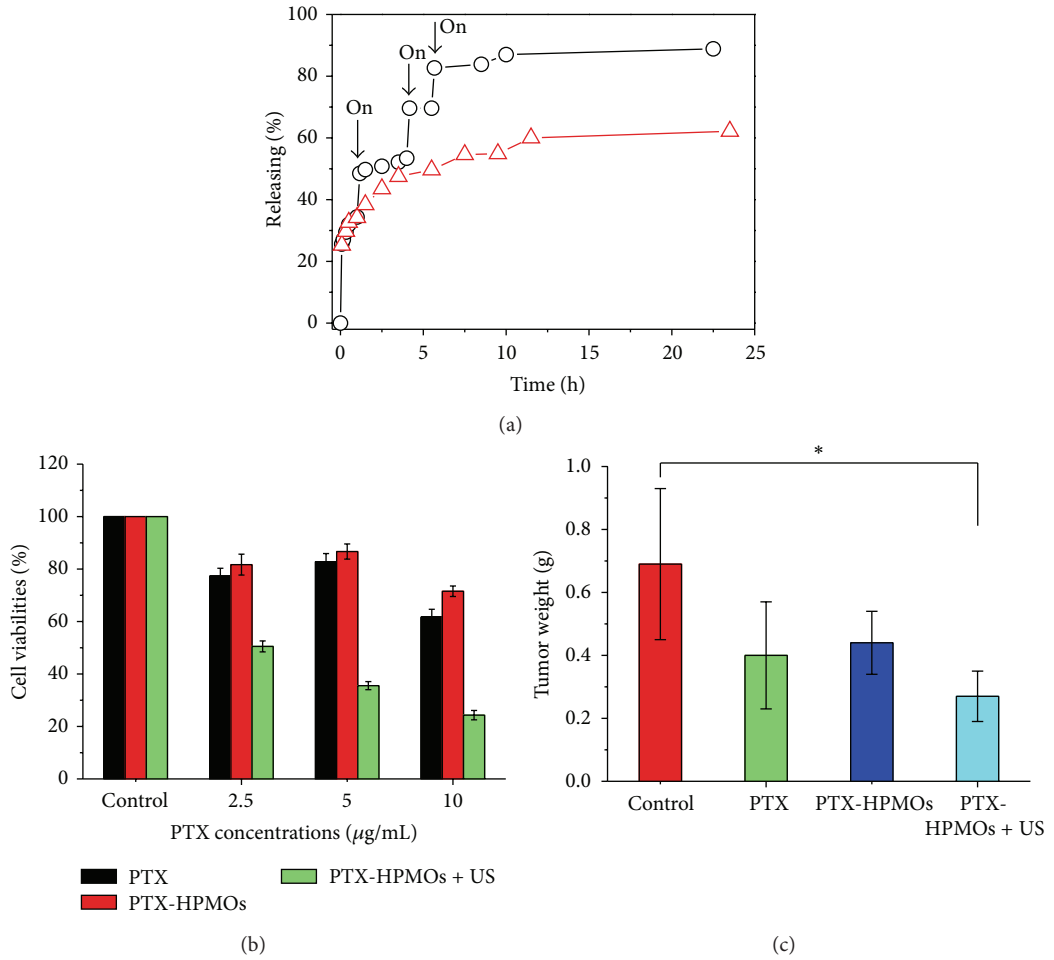

FIGURE 3: (a) *In vitro* PTX releasing from PTX-loaded HPMOs in PBS solution with (black line) and without (red line) ultrasound irradiation; (b) average cell viabilities ($n = 3$) of each treatment against HeLa cells at different concentrations for 24 h; (c) tumor weight after the administration of saline solution (control), free PTX, PTX-HPMOs, and PTX-HPMOs + US ($^*P < 0.05$).

the organosilica precursors. The silica core is less condensed compared to PMO shell; thus, it can be easily etched away by alkaline etching. Figure 1 shows that the PMOs shell can perfectly remain after the mild etching in 0.6 M Na_2CO_3 solution at 80°C for 1 h. The obtained HPMOs show the uniform spherical morphology and high dispersity, which are very beneficial for further *in vivo* theranostic applications. The hollow nanostructures can be demonstrated by the contrast differences between the core and shell in TEM image (Figure 1(a)). The ordered and well-defined mesoporous channels within the PMOs shell can be clearly distinguished in TEM image with high magnification (Figure 1(b)). In addition, SEM image also demonstrates that obtained HPMOs possess spherical morphology and high dispersity (Figure 1(c)). The particle size of HPMOs is 450.2 nm. In addition, the surface area, pore volume, and pore size of HPMOs are 1029.4 m^2/g, 0.66 cm^3/g, and 2.8 nm, respectively [25].

Furthermore, we systematically evaluated the *in vitro* acoustic enhancement of HPMOs under different concentrations, ultrasound imaging modalities, and mechanical indexes. The typical ultrasonography images were obtained under both harmonic imaging mode and conventional contrast mode in the presence of HPMOs. It is interesting that the introduction of HPMOs exhibits the obvious contrast enhancement under both harmonic and B-modes, and this special grayscale imaging enhancement is strongly dependent on the HPMOs concentrations and mechanical indexes (Figures 2(a)–2(l) and Figure S1; see supplementary Figure S1 in Supplementary Material available online at http://dx.doi.org/10.1155/2014/972475). This result indicated that the contrast enhancement generated by the introduction of HPMOs is very stable under high mechanical indexes because the adopted mechanical indexes of harmonic mode are between 0.6 and 1.2, while the commercial SonoVue suffers from the rapture of microbubbles under high mechanical indexes and only can image under low mechanical indexes of contrast mode. This phenomenon further demonstrates the high stability of HPMOs for ultrasonography. The quantitative measurement of the gray values of ultrasound imaging using HPMOs as the CAs further demonstrates that the HPMOs can significantly enhance the responsiveness of

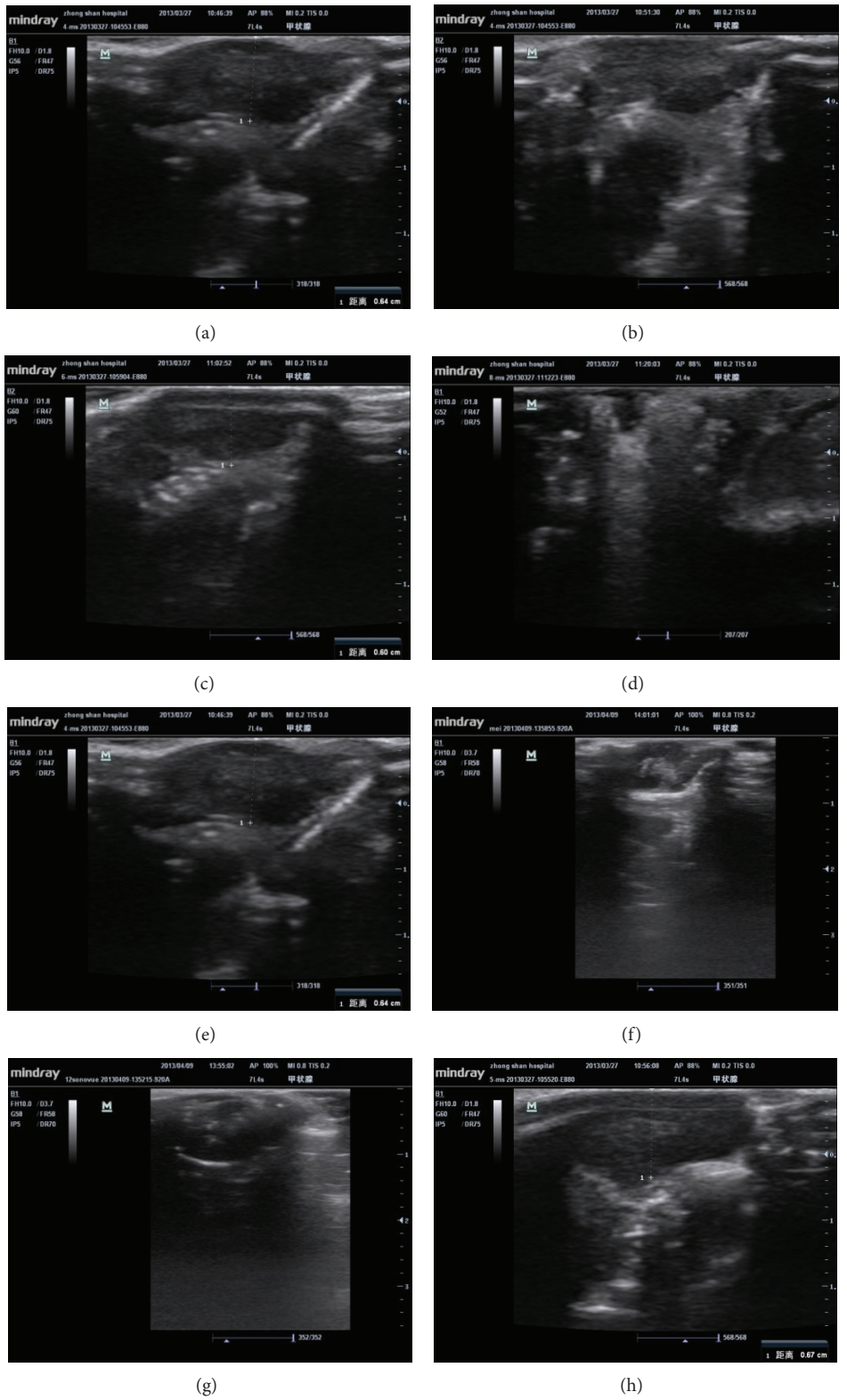

(a) (b)

(c) (d)

(e) (f)

(g) (h)

Figure 4: *In vivo* ultrasound imaging of tumor-bearing mice before ((a), (c), and (e)) and after ((b), (d), and (f)) the administration of different contrast agents: saline solution (a and b), PTX-HPMOs (c and d), and SonoVue (e and f). Images (g) and (h) represent tumor ultrasound images after 7 days of administration of PTX-HPMOs (g) and SonoVue (h).

HPMOs of ultrasound and generate the contrast enhancement of ultrasound imaging. Importantly, both HPMOs and SonoVue show good effect of contrast-enhanced ultrasound imaging under contrast mode (Figure S2).

We further used HPMOs as the drug delivery system (DDS) for ultrasound-triggered drug release and delivery due to the unique hollow interiors and mesoporous shell, which could largely protect the healthy organs from the toxic drugs and prevent the decomposition/denaturing of the drugs prior to reaching the targeted tissue [26–28]. The large hollow interiors leave much more room for drug molecules and the mesoporous channels provide diffusion pathways [29]. Paclitaxel (PTX), a typical hydrophobic anticancer drug, was encapsulated within HPMOs. The drug loading amount is as high as 90.9 mg/g, which is higher than traditional mesoporous silica nanoparticles due to the contribution of large hollow interior of HPMOs [30]. Importantly, it was found that the PTX releasing profile was biphasic, with an initial abrupt release followed by sustained and slow release without ultrasound irradiation. Abrupt release occurred at 5 min, and 23% of the loaded PTX was released by that time. Then, the release of PTX showed sustained and slow release following the initial abrupt release. After 12 h, 40% of the loaded PTX was still enveloped within HPMOs and the release enters into the plateau. Comparatively, under ultrasound irradiation, the PTX release profile can be controlled by ultrasound irradiation. Ultrasound irradiation can enhance about 18% of the PTX release every time. After 3 times of ultrasound irradiation, the release of PTX reached 82.2% at 5.5 h (Figure 3(a)). This result demonstrates that PTX-loaded HPMOs exhibit ultrasound-triggered drug releasing performances and could be used in ultrasonic-assisted chemotherapy of cancer. The unique organic benzene groups within the framework of HPMOs can interact with PTX molecules through supramolecular π-π stacking, which can be disrupted by external ultrasound triggers to cause the ultrasound-based stimuli-responsive drug releasing.

The *in vitro* ultrasound-triggered drug releasing behavior of PTX-HPMOs was further investigated on human cervical cancer HeLa cell line. It was found that (Figure 3(b)) the loaded PTX with ultrasound irradiation can exhibit higher cytotoxicity at PTX concentrations of 2.5, 5, and 10 μg/mL. When the concentration of PTX was 5 μg/mL, there was 35.56% cell survival, but with the further increase of PTX concentrations up to 10 μg/mL, more than 75.69% of HeLa cells were killed. However, pure ultrasound irradiation has no obvious cytotoxicity. Thus, ultrasound irradiation could enhance the release of PTX from PTX-containing nanocapsules, which should be responsible for the higher concentration of PTX in the cell, leading to the enhanced PTX cytotoxicity and cell death. Moreover, the cavitation effect of ultrasound may also promote the tumor cell death.

The *in vivo* ultrasound-triggered drug releasing behavior of PTX-HPMOs was investigated on tumor-bearing mice. It was found (Figure 3(c)) that PTX-HPMOs with ultrasound irradiation exhibit significantly higher tumor inhibition rate (61%) compared to free PTX (42%) and PTX-HPMOs (36%). We also observed the large necrosis of tumor tissues in PTX-HPMOs combined with ultrasound group. Therefore, the combined ultrasound-triggered drug releasing and ultrasound-based cavitation effect cause this high therapeutic efficiency.

Importantly, HPMOs can be used as the CAs for ultrasound imaging during the chemotherapeutic process. The PTX-loaded HPMOs were intratumorally injected and noninvasively detected by ultrasound at different time intervals (Figure 4 and Figure S3). It was found that the tumor tissues exhibited obvious contrast enhancement in ultrasonography image after the administration of HPMOs (Figures 4(c) and 4(d)), which could diffuse rapidly within tumor tissue. It is indicated that the PTX-HPMOs' diameter between 400 and 500 nm can overcome the drawback of particle size of organic microbubbles and can pass through the link of the capillaries of tumor tissue to diffuse rapidly within tumor tissues. Importantly, HPMOs exhibit higher *in vivo* stability than commercial clinically used SonoVue (Figures 4(e), 4(f), 4(g), and 4(h) and Figure S3). The contrast enhancement remained even after 7 days in PTX-HPMOs group, while the SonoVue did not show such effect. These results show that HPMOs can also be used for real-time *in vivo* ultrasound imaging for the determination of the progress of lesion tissues during chemotherapeutic process and can release the anticancer drugs persistently for efficient chemotherapy.

4. Conclusions

In summary, novel molecularly organic/inorganic hybrid hollow mesoporous periodic organosilica nanoparticles were elaborately designed and prepared by a typical hard-templating method, which were further systematically investigated as the efficient CAs for *in vitro* and *in vivo* ultrasound imaging and simultaneous ultrasound-triggered drug delivery systems. HPMOs exhibited excellent *in vitro* and *in vivo* performances in contrast-enhanced ultrasonography and could be used for the *in situ* determination of the progress of lesion tissues during the chemotherapeutic process. Importantly, PTX-loaded HPMOs combined with ultrasound irradiation showed ultrasound responsiveness and higher tumor inhibition rates compared with free PTX and PTX-HPMOs, which was due to the ultrasound-triggered drug release and ultrasound-induced cavitation effect. It is believed that the achieved novel HPMOs will find great application potentials in clinically ultrasound-based imaging and therapy.

Conflict of Interests

The authors declare that there is no conflict of interests regarding the publication of this paper.

Acknowledgments

The authors greatly acknowledge the financial support from the Foundation for Youth Scholar of State Key Laboratory of High Performance Ceramics and Superfine Microstructure (Grant no. SKL201203), the National Natural Science Foundation of China (Grants nos. 51302293 and 81371577), the Natural Science Foundation of Shanghai (13ZR1463500), and

the Science and Technology Support Plan of Zhenjiang City (SH2013080).

References

[1] E. G. Schutt, D. H. Klein, R. M. Mattrey, and J. G. Riess, "Injectable microbubbles as contrast agents for diagnostic ultrasound imaging: the key role of perfluorochemicals," *Angewandte Chemie*, vol. 42, no. 28, pp. 3218–3235, 2003.

[2] W. B. Cai and X. Y. Chen, "Nanoplatforms for targeted molecular imaging in living subjects," *Small*, vol. 3, no. 11, pp. 1840–1854, 2007.

[3] J. A. Feshitan, F. Vlachos, S. R. Sirsi, E. E. Konofagou, and M. A. Borden, "Theranostic Gd(III)-lipid microbubbles for MRI-guided focused ultrasound surgery," *Biomaterials*, vol. 33, no. 1, pp. 247–255, 2012.

[4] B. E. Oeffinger and M. A. Wheatley, "Development and characterization of a nano-scale contrast agent," *Ultrasonics*, vol. 42, no. 1–9, pp. 343–347, 2004.

[5] H. Alkan-Onyuksel, S. M. Demos, G. M. Lanza et al., "Development of inherently echogenic liposomes as an ultrasonic contrast agent," *Journal of Pharmaceutical Sciences*, vol. 85, no. 5, pp. 486–490, 1996.

[6] M. A. Borden, H. Zhang, R. J. Gillies, P. A. Dayton, and K. W. Ferrara, "A stimulus-responsive contrast agent for ultrasound molecular imaging," *Biomaterials*, vol. 29, no. 5, pp. 597–606, 2008.

[7] P. Lin, R. J. Eckersley, and E. A. H. Hall, "Ultra bubble: a laminated ultrasound contrast agent with narrow size range," *Advanced Materials*, vol. 21, no. 38-39, pp. 3949–3952, 2009.

[8] Y. Chen, Q. Yin, X. F. Ji et al., "Manganese oxide-based multifunctionalized mesoporous silica nanoparticles for pH-responsive MRI, ultrasonography and circumvention of MDR in cancer cells," *Biomaterials*, vol. 33, no. 29, pp. 7126–7137, 2012.

[9] H. Hu, H. Zhou, J. Du et al., "Biocompatiable hollow silica microspheres as novel ultrasound contrast agents for *in vivo* imaging," *Journal of Materials Chemistry*, vol. 21, no. 18, pp. 6576–6583, 2011.

[10] M. A. Malvindi, A. Greco, F. Conversano et al., "Magnetic/silica nanocomposites as dual-mode contrast agents for combined magnetic resonance imaging and ultrasonography," *Advanced Functional Materials*, vol. 21, no. 13, pp. 2548–2555, 2011.

[11] X. Wang, H. Chen, Y. Chen et al., "Perfluorohexane-encapsulated mesoporous silica nanocapsules as enhancement agents for highly efficient high intensity focused ultrasound (HIFU)," *Advanced Materials*, vol. 24, no. 6, pp. 785–791, 2012.

[12] H. P. Martinez, Y. Kono, S. L. Blair et al., "Hard shell gas-filled contrast enhancement particles for colour Doppler ultrasound imaging of tumors," *MedChemComm*, vol. 1, no. 4, pp. 266–270, 2010.

[13] F. Tang, L. Li, and D. Chen, "Mesoporous silica nanoparticles: synthesis, biocompatibility and drug delivery," *Advanced Materials*, vol. 24, no. 12, pp. 1504–1534, 2012.

[14] N. E. Botterhuis, Q. Y. Sun, P. Magusin, R. A. van Santen, and N. Sommerdijk, "Hollow silica spheres with an ordered pore structure and their application in controlled release studies," *Chemistry*, vol. 12, no. 5, pp. 1448–1456, 2006.

[15] D. Chen, N. Li, F. Tang, and S. Qi, "Facile and scalable synthesis of tailored silica "nanorattle" structures," *Advanced Materials*, vol. 21, no. 37, pp. 3724–3807, 2009.

[16] H. M. Chen, J. H. He, H. M. Tang, and C. X. Yan, "Porous silica nanocapsules and nanospheres: dynamic self-assembly synthesis and application in controlled release," *Chemistry of Materials*, vol. 20, no. 18, pp. 5894–5900, 2008.

[17] X. Fang, C. Chen, Z. Liu, P. Liu, and N. Zheng, "A cationic surfactant assisted selective etching strategy to hollow mesoporous silica spheres," *Nanoscale*, vol. 3, no. 4, pp. 1632–1639, 2011.

[18] T. Kim, E. Momin, J. Choi et al., "Mesoporous silica-coated hollow manganese oxide nanoparticles as positive T 1 contrast agents for labeling and MRI tracking of adipose-derived mesenchymal stem cells," *Journal of the American Chemical Society*, vol. 133, no. 9, pp. 2955–2961, 2011.

[19] T. Liu, L. Li, X. Teng et al., "Single and repeated dose toxicity of mesoporous hollow silica nanoparticles in intravenously exposed mice," *Biomaterials*, vol. 32, no. 6, pp. 1657–1668, 2011.

[20] T. Wang, L. Zhang, Z. Su, C. Wang, Y. Liao, and Q. Fu, "Multifunctional hollow mesoporous silica nanocages for cancer cell detection and the combined chemotherapy and photodynamic therapy," *ACS Applied Materials and Interfaces*, vol. 3, no. 7, pp. 2479–2486, 2011.

[21] M. S. Yavuz, Y. Cheng, J. Chen et al., "Gold nanocages covered by smart polymers for controlled release with near-infrared light," *Nature Materials*, vol. 8, no. 12, pp. 935–939, 2009.

[22] Y. Chen, H. Chen, and J. Shi, "In vivo bio-safety evaluations and diagnostic/therapeutic applications of chemically designed mesoporous silica nanoparticles," *Advanced Materials*, vol. 25, no. 23, pp. 3144–3176, 2013.

[23] J. Shi, Y. Chen, and H. Chen, "Progress on the multifunctional mesoporous silica-based nanotheranostics," *Journal of Inorganic Materials*, vol. 28, no. 1, pp. 1–11, 2013.

[24] C. Urata, H. Yamada, R. Wakabayashi et al., "Aqueous colloidal mesoporous nanoparticles with ethenylene-bridged silsesquioxane frameworks," *Journal of the American Chemical Society*, vol. 133, no. 21, pp. 8102–8105, 2011.

[25] Y. Chen, P. Xu, H. Chen et al., "Colloidal HPMO nanoparticles: Silica-etching chemistry tailoring, topological transformation, and nano-biomedical applications," *Advanced Materials*, vol. 25, no. 22, pp. 3100–3105, 2013.

[26] Y. Chen, H.-R. Chen, and J.-L. Shi, "Construction of homogenous/heterogeneous hollow mesoporous silica nanostructures by silica-etching chemistry: principles, synthesis, and applications," *Accounts of Chemical Resea*, vol. 47, no. 1, pp. 125–137, 2013.

[27] Y. Chen, C. Chu, Y. C. Zhou et al., "Reversible pore-structure evolution in hollow silica nanocapsules: large pores for siRNA delivery and nanoparticle collecting," *Small*, vol. 7, no. 20, pp. 2935–2944, 2011.

[28] Y. Chen, H. Chen, Y. Sun et al., "Multifunctional mesoporous composite nanocapsules for highly efficient MRI-guided high-intensity focused ultrasound cancer surgery," *Angewandte Chemie-International Edition*, vol. 50, no. 52, pp. 12505–12509, 2011.

[29] Y. Chen, H. R. Chen, L. M. Guo et al., "Hollow/rattle-type mesoporous nanostructures by a structural difference-based selective etching strategy," *ACS Nano*, vol. 4, no. 1, pp. 529–539, 2010.

[30] J. Lu, M. Liong, J. I. Zink, and F. Tamanoi, "Mesoporous silica nanoparticles as a delivery system for hydrophobic anticancer drugs," *Small*, vol. 3, no. 8, pp. 1341–1346, 2007.